CHARACTERIZATION OF MICRO-PERFORATED MATERIALS

Felicitas Spörk[1], Dominik Mayrhofer[1], Manfred Kaltenbacher[1]

[1] *Institute of Fundamentals and Theory in Electrical Engineering, TU Graz, Austria*

Abstract

Micro-perforated plates (MPPs) are thin plates containing perforations in the submillimeter range. As the incident sound wave penetrates the material, energy is dissipated by friction in the perforations. In this study, the acoustic mechanisms in micro-perforated plates and foils are investigated. Due to different manufacturing techniques, the investigated materials exhibit different perforation geometries: circular and slitted perforations. To characterize the materials' absorption behavior, measurements in the impedance tube are performed. Using optimization techniques, the parameters of theoretical models, such as the Maa model, can be obtained. Furthermore, a cost function is defined to optimize the absorption in a specified frequency range using the material parameters and the geometry as design variables. Since the investigations cover circular and slitted plates, the latter require a more in-depth analysis since the Maa model assumes a circular geometry. Here, numerical simulations using the finite element method are employed to accurately model the absorption via a unit cell of the micro-perforated plate. The numerical computations are based on the linearized compressible flow equations to investigate the viscous dissipation mechanism in depth. Comparisons with measurements suggest that the unit cell simulations can predict the absorption behavior of the micro-perforated plates well and efficiently, also for more complex slit geometries.

Keywords: *MPP, FEM, optimization, chain matrices*

1. Introduction

A micro-perforated plate (MPP) is a thin plate with perforations in the submillimeter range that can be used for sound absorption, and they are an alternative to porous absorber materials. The working principle are viscous and thermal losses of air inside the tiny perforations. Figure 1 shows a MPP absorber with the orifice diameter d, the panel thickness t, the distance between holes b and the air cavity depth D between backing wall and panel.

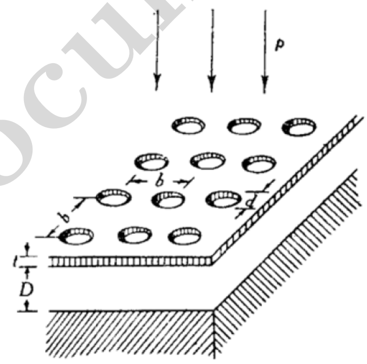

Figure 1: Sketch of micro-perforated panel absorber (MPA) according to [1].

1.1. Maa model

Maa introduced an impedance model for micro-perforated plates [2]. This model has a resistive part which describes the energy loss, hence the viscous dissipation within the perforations and a reactive part which describes the mass effect of air in holes

$$\begin{aligned} \underline{Z}_{\mathrm{MPP}}(f) &= R + j\omega M = \rho_0 c_0 (r + j\omega m) \\ r &= \frac{32\eta t}{\phi \rho_0 c_0 d^2}\left(\sqrt{1+\frac{k_\mathrm{p}^2}{32}} + \frac{\sqrt{2}}{32} k_\mathrm{p} \frac{d}{t}\right) \\ m &= \frac{t}{\phi c_0}\left(1 + \frac{1}{\sqrt{9+\frac{k_\mathrm{p}^2}{2}}} + 0.85\frac{d}{t}\right), \end{aligned} \quad (1)$$

with the perforate constant k_p and the angular frequency ω being

$$k_\mathrm{p} = d\sqrt{\frac{\omega \rho_0}{4\eta}}, \quad \omega = 2\pi f. \quad (2)$$

Corresponding author: *felicitas.spoerk@tugraz.at.*

In Eq. (1) and (2) t denotes the panel thickness, d the hole diameter, ϕ the perforation ratio, η the dynamic viscosity of air, ρ_0 the air density, c_0 the speed of sound and f the frequency.
The perforation ratio is the ratio between open area and total area. For a 60-degree staggered perforation pattern with circular holes, as displayed in Fig. 2, we can calculate the perforation ratio with

$$\phi = \frac{A_{\text{hole}}}{A_{\text{cell}}} = \frac{\pi\left(\frac{d}{2}\right)^2}{\sin(60^\circ)p^2} = \frac{\pi\left(\frac{d}{2}\right)^2}{\frac{\sqrt{3}}{2}p^2} = \frac{\pi d^2}{2\sqrt{3}p^2}, \quad (3)$$

where p is the distance between holes.

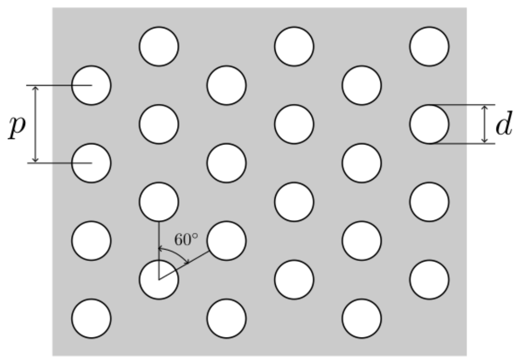

Figure 2: 60-degree staggered perforation pattern with circular holes.

The absorption coefficient of a MPP absorber (MPA) can be measured in the impedance tube (see Fig 3). In the schematic, the air cavity depth behind the MPP is denoted by L_c and the distance between the two microphones is denoted as d_mic.

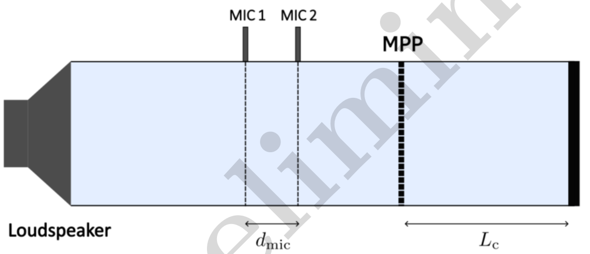

Figure 3: Setup for absorption coefficient measurements with the two-microphone method using an impedance tube.

2. Multi-layered structures

The MPA can be analytically described using chain matrices [3]. The description with chain matrices also enables the design of MPAs using multiple MPPs and cavities. The material parameters of the MPP can be identified by fitting the predicted absorption coefficient to the measured absorption spectrum.

2.1. Parameter fitting

The micro-perforated panel impedance with the material parameters t, d and ϕ is calculated using Maa's model (1). The chain matrix of the MPP is represented as a lumped shunt element, where the velocity is continuous and the pressure jumps. The backing cavity is described by the transfer matrix of an air layer. The total chain matrix for the absorber structure is therefore

$$\begin{aligned}\underline{\boldsymbol{T}}_\text{total} = \underline{\boldsymbol{T}}_\text{MPP}\underline{\boldsymbol{T}}_\text{air} &= \begin{bmatrix} A & B \\ C & D \end{bmatrix} \quad (4)\\ &= \begin{bmatrix} 1 & \underline{Z}_\text{MPP} \\ 0 & 1 \end{bmatrix} \begin{bmatrix} \cos(kL_\text{c}) & jZ_0 \sin(kL_\text{c}) \\ j\dfrac{1}{Z_0}\sin(kL_\text{c}) & \cos(kL_\text{c}) \end{bmatrix},\end{aligned}$$

where k is the acoustic wavenumber and Z_0 is the characteristic impedance of air

$$k = \frac{\omega}{c_0}, \quad (5)$$

$$Z_0 = \rho_0 c_0. \quad (6)$$

The transfer matrix relates the acoustic pressure and particle velocity at the front surface of the absorber to those at the back surface. We know, that the particle velocity is zero at a rigid termination. Consequently, we obtain

$$\begin{bmatrix} \underline{p}_\text{front} \\ \underline{v}_\text{front} \end{bmatrix} = \underline{\boldsymbol{T}}_\text{total} \begin{bmatrix} \underline{p}_\text{back} \\ \underline{v}_\text{back} \end{bmatrix} = \begin{bmatrix} A & B \\ C & D \end{bmatrix} \begin{bmatrix} \underline{p}_\text{back} \\ 0 \end{bmatrix}, \quad (7)$$

which yields the input acoustic impedance $\underline{Z}_\text{in}$, which is the ratio of pressure and velocity directly in front of the MPP

$$\underline{Z}_\text{in} = \frac{\underline{p}_\text{front}}{\underline{v}_\text{front}} = \frac{A}{C}. \quad (8)$$

The reflection can be determined with the impedances

$$\underline{r} = \frac{\underline{Z}_\text{in} - Z_0}{\underline{Z}_\text{in} + Z_0}. \quad (9)$$

Finally, with the reflection factor the absorption coefficient α can be calculated

$$\alpha = 1 - |\underline{r}|^2. \quad (10)$$

The absorption coefficient is used in the fitting for the comparison to the measurements. The calculated absorption spectrum was interpolated onto the measured frequency points. The material parameters t, d, and ϕ were identified by minimizing the sum of squared errors between the measured absorption coefficient α_meas and predicted absorption coefficients α_model using the differential evolution algorithm. The objective reads as

$$J(\boldsymbol{x}) = \sum_{i=1}^{N} \left[\alpha_\text{model}(f_i;\boldsymbol{x}) - \alpha_\text{meas}(f_i)\right]^2, \quad (11)$$

where $\boldsymbol{x} = [t, d, \phi]$ is the parameter vector, N denotes

the number of measured frequency points and f_i the corresponding measurement frequencies.
The absorption of different MPP samples was characterized in the impedance tube. To demonstrate the fitting of parameters, we look at a fabricated MPP, where laser technology was used to obtain small, almost circular perforation holes as shown in Fig. 4.

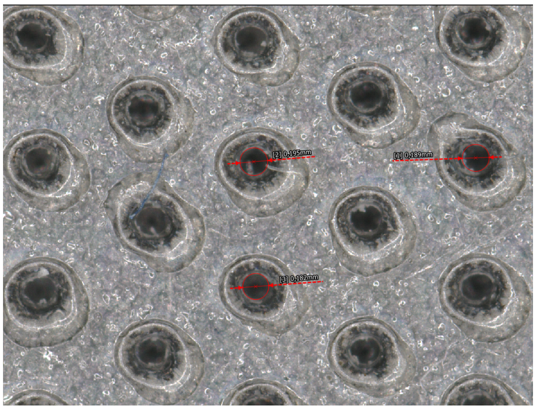

Figure 4: Laser perforated foil.

Figure 5 shows the measurements and the fitting result for the lasered foil with a thickness of 280 μm and 7 cm air cavity. The parameters which were obtained from the optimization are listed in Table 1. We see that good agreement between the measured and computed results can be obtained.

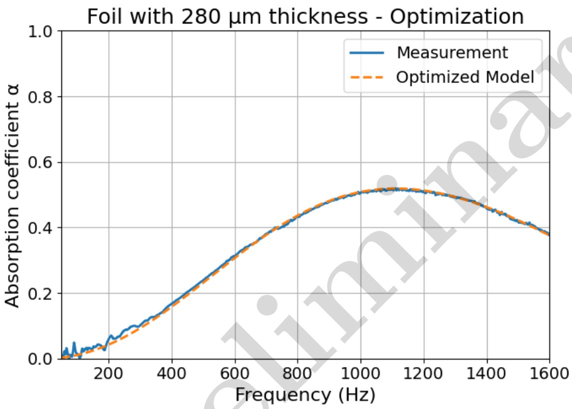

Figure 5: Parameter fitting for the measurement results of the lasered foil with thickness 280 μm with 7 cm air cavity depth.

Table 1: Parameters obtained from the optimization. Lasered foil with 280 μm thickness and 7 cm air cavity.

thickness t	*diameter d*	*perforation ratio ϕ*
0.26 mm	0.197 mm	5.98 %

2.2. Layered Model

An optimization study was performed using chain matrices for the modeling to determine a multiple MPA design which is capable of providing sound absorption performance particularly at low frequencies. The optimization considered both the geometric variables and the parameters of the Maa model. The resulting optimal design comprised three MPPs, each featuring different perforation ratios and cavities of varying depths from one another and from the rigid backing. In the shown case, the thickness and hole diameter of the MPPs were not varied. Instead, the fitted parameters of the foil were used (see Table 1). This layered configuration enhances acoustic energy dissipation by combining the viscous loss mechanism with multiple resonant interactions, thereby increasing the frequency range over which effective sound absorption is achieved. In Fig. 6, the resulting absorption performance is shown and Table 2 lists the optimized design parameters.

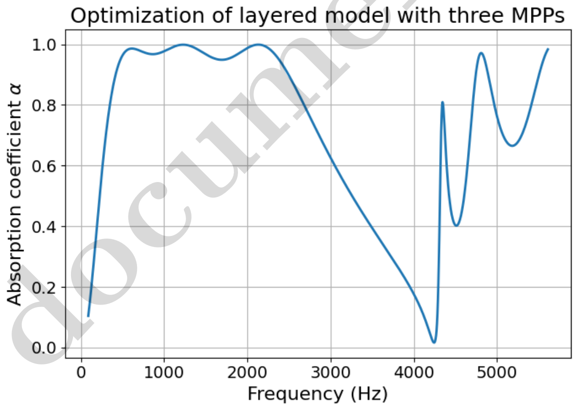

Figure 6: Absorption of the optimization results for a layered model with three MPPs.

Table 2: Parameters of the optimized multilayer absorber.

Parameter	*Value*
t_1	0.26 mm
d_1	0.197 mm
ϕ_1	3.223 %
t_2	0.26 mm
d_2	0.197 mm
ϕ_2	1.744 %
t_3	0.26 mm
d_3	0.197 mm
ϕ_3	0.663 %
d_{12}	39.02 mm
d_{23}	40.26 mm
$d_{3\mathrm{b}}$	40.69 mm

3. Towards slitted MPAs

Commercially manufactured MPPs are generally fabricated using mechanical processing techniques, including punching, milling, or plastic forming methods. The resulting perforations are often slit-shaped rather than cylindrical. This perforation geometry differs from the assumptions underlying many theoretical models, which typically consider circular holes. Figure 7 shows a material sample with slit-shaped apertures.

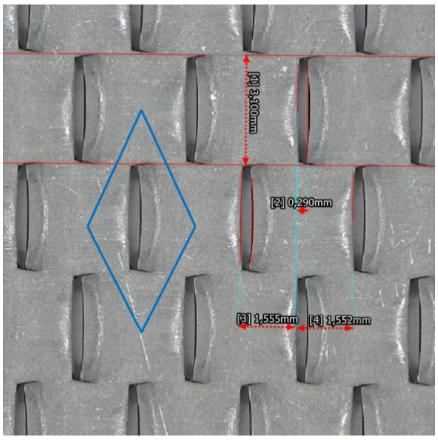

Figure 7: Material sample with slit-shaped perforation.

To investigate slitted MPAs analytically, Maa's model can be employed [4]. The impedance for a slitted MPA is given by

$$\begin{aligned}\underline{Z}_{\mathrm{MPP,slit}}(f) &= R + j\omega M = \rho_0 c_0 (r + j\omega m)\\ r &= \frac{12\eta t}{\phi \rho_0 c_0 d^2}\left(\sqrt{1+\frac{k_{\mathrm{p}}^2}{18}} + \frac{\sqrt{2}}{12} k_{\mathrm{p}} \frac{d}{t}\right)\\ m &= \frac{t}{\phi c_0}\left(1 + \frac{1}{\sqrt{5^2 + 2k_{\mathrm{p}}^2}} + \frac{F(e)}{2}\frac{d}{t}\right),\end{aligned} \tag{12}$$

based on Maa's original publication [4]. Here, $F(e)$ is the complete elliptic integral of the first kind. The end-correction can play a major role and must be adapted from Maa's original model to incorporate an MPA's rounded or sharp edges [5], [6]. Generalizing the end-correction term and using the end-correction coefficient $\alpha_{\mathrm{E}} = 2,4$ for rounded or sharp edges based on [6] results in a reactive term of the form

$$r = \frac{12\eta t}{\phi \rho_0 c_0 d^2}\left(\sqrt{1+\frac{k_{\mathrm{p}}^2}{18}} + \frac{\sqrt{2}\,\alpha_{\mathrm{E}}}{6} k_{\mathrm{p}} \frac{d}{t}\right). \tag{13}$$

In Eq. (13) α_{E} denotes a free parameter that can be used to adapt the model to the actual manufacturing method. Additionally, the given parameters for sharp and rounded edges can deviate for MPAs with very small slits due to overlapping boundary layers. Here, FEM simulations can be used to fine-tune the model.

3.1. Numerical Simulation of a Unit Cell

As presented in [7], a numerical unit cell simulation using the finite element method (FEM) is employed to model the absorption of the slitted MPP. The unit cell includes a single slit (see Fig. 7). The numerical computations are based on the linearized compressible flow equations to model the viscous dissipation mechanism within the perforation. The open source software *openCFS* [8] was used for all simulations. Evaluating the validity of this approach is particularly of interest because it assumes that the acoustic response of an entire MPP can be accurately described using a periodic unit-cell model, despite the deviations from idealized perforation geometries and the possibility of interaction effects between adjacent slits. In the simulation, the slit was assumed to be ideally rectangular. Figure 8 shows the simulation geometry. The geometry matches that of the impedance tube. On the surface Γ_{excite} a normal velocity is defined as excitation. The no-slip boundary condition is defined at all surfaces that would have contact with the material.

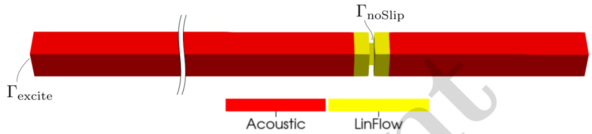

Figure 8: Simulation geometry of the unit cell.

To significantly reduce the computational load, we solve the linearized compressible flow equations just in the slit and its surrounding region and then couple to the classical wave equation [9].
In Fig. 9 the resulting fluid velocity distribution within the slit is displayed. In the vicinity of the slit boundaries, the velocity amplitude is amplified before rapidly decreasing to zero at the wall due to the no-slip boundary condition. This behavior indicates the formation of a viscous boundary layer, where pronounced velocity gradients are present. These gradients enhance viscous losses, which have a crucial role in the mechanism of acoustic energy absorption in micro-perforated structures.

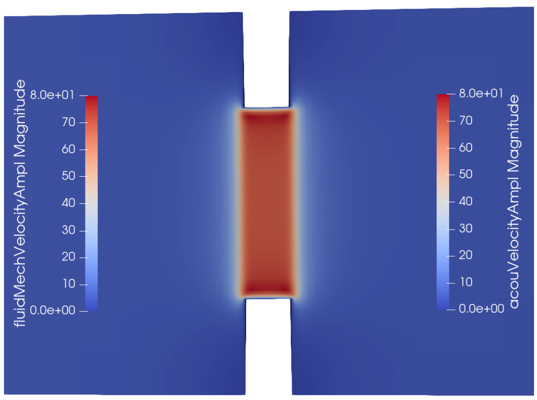

Figure 9: Fluid velocity distribution in the slit.

Numerical simulations were performed over a broad frequency range and the acoustic absorption was calculated applying the same method used in impedance tube measurements. Figure 10 shows the comparison between the numerically predicted and measured absorption coefficient. The slit is not ideally rectangular but is rather arched. Therefore, the slit width is reduced to account for this effect. Adjusting the slit width slightly in the numerical model, leads to an even better agreement between the simulated and experimental results. There are deviations, but the overall frequency-dependent behavior is quite well captured with the unit-cell simulation.

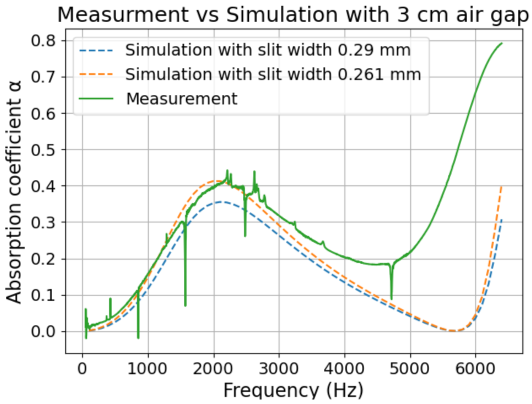

Figure 10: Comparison of the absorption coefficient over frequency with 3 cm cavity depth.

3.2. Comparison to the analytical model

Based on the FEM simulations, the parameter α_{E} has been fitted to accurately model the end correction for this case. Over six different simulations, it has been found that the ideal value for the coefficient is given by $\alpha_{\mathrm{E}} = 2.2$, lying in the original range of 2 to 4. Based on this result, the absorption curve of the MPA has been evaluated and is depicted in Fig. 11.

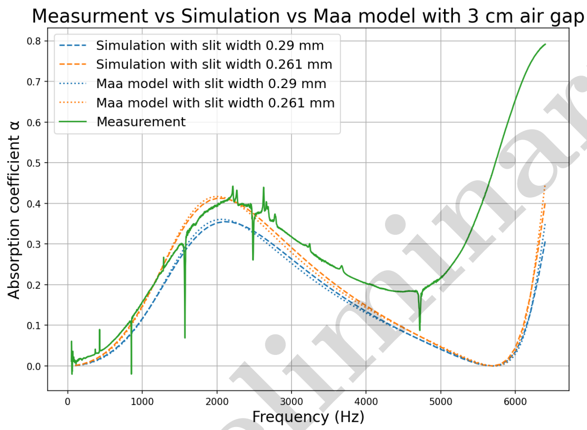

Figure 11: Comparison of the absorption coefficient over frequency with 3 cm cavity depth including Maa's adapted model.

As it can be seen, the fine-tuned model agrees with the FEM simulation very well. For similar arrangements, the tuned analytical model can be used to replace the FEM model with little loss of accuracy and comparably negligible computational cost. It has to be noted though that it seems that both the analytical model as well as the FEM model are lacking a physical absorption mechanism that is present in the measurements. This is especially relevant for the local minima of the absorption curve, where the numerical models tend towards zero, whereas the measurements show some residual absorption.

4. Conclusion

This contribution demonstrates the effectiveness of multilayer micro-perforated absorbers (MPAs) for achieving broadband sound absorption. For the design of the model and for parameter fitting to measurements, the chain matrix method was used. For the characterization of a slitted micro-perforated plate (MPP), numerical simulations were performed. Comparisons with measurements suggest that the unit-cell simulations can predict the absorption behavior of the MPP well and efficiently, also for more complex slit geometries. The simulation results are also compared to an analytical model, which is a modified version of Maa's original model. It can be observed that the analytical model and the simulation results agree very well. Therefore, the analytical model can replace the simulation in this case and for similar arrangements, which reduces the computational cost. The residual disagreement of the low-absorption region is most likely caused by a missing effect in the simulation as well as the analytical model and needs further investigation.

References

[1] D.-Y. Maa, "Theory and design of microperforated panel sound-absorbing constructions," *Scientia Sinica*, 1975.

[2] D.-Y. Maa, "Potential of microperforated panel absorber," *The Journal of the Acoustical Society of America*, vol. 104, no. 5, pp. 2861–2866, 1998. DOI: `10.1121/1.423870`.

[3] W. Truppe and F. Kappler, "Messsystem für akustische zweitore," Master's thesis, Technische Universität Graz, Austria, 2008.

[4] D.-Y. Maa, "Theory of microslit absorbers," *Acta Acustica (Chinese)*, vol. 25, no. 6, pp. 481–485, 2000. DOI: `10.15949/j.cnki.0371-0025.2000.06.001`.

[5] U. Ingard, "On the theory and design of acoustic resonators," *J. Acoust. Soc. Am.*, vol. 25, no. 6, pp. 1037–1061, 1953. DOI: `10.1121/1.1907235`.

[6] F. Auriemma, "Acoustic performance of micro-grooved elements," *Applied Acoustics*, vol. 122, pp. 128–137, 2017. DOI: `10.1016/j.apacoust.2017.02.019`.

[7] M. Kaltenbacher, F. Spörk, and D. Mayrhofer, "Investigation of the acoustic mechanism in micro-perforated-plates," 2026. DOI: `10.71568/daga2026.534`.

[8] "Open source software *openCFS*: Finite elements for multiphysics," Accessed: Jul. 30, 2026. [Online]. Available: `http://opencfs.org`.

[9] D. Mayrhofer, K. Roppert, D. Tumpold, and M. Kaltenbacher, "A moving mesh method for fluid-solid-acoustic interactions in mems devices," *Journal of Theoretical and Computational Acoustics*, 2024. DOI: `10.1142/S2591728524500166`.